



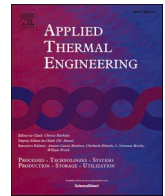
Feasibilities of utilizing thermal inertia of district heating networks to improve system flexibility

Downloaded from: <https://research.chalmers.se>, 2025-12-06 04:17 UTC

Citation for the original published paper (version of record):

Zhang, Y., Johansson, P., Sasic Kalagasidis, A. (2022). Feasibilities of utilizing thermal inertia of district heating networks to improve system flexibility. *Applied Thermal Engineering*, 213.
<http://dx.doi.org/10.1016/j.applthermaleng.2022.118813>

N.B. When citing this work, cite the original published paper.



Feasibilities of utilizing thermal inertia of district heating networks to improve system flexibility

Yichi Zhang^{*}, Pär Johansson, Angela Sasic Kalagasidis

Department of Architecture and Civil Engineering, Division of Building Technology, Chalmers University of Technology, Gothenburg 412 96, Sweden

ARTICLE INFO

Keywords:

District heating
Network inertia
Thermal energy storage
Wind power integration
Combined heat and power

ABSTRACT

The use of district heating network inertia (DHNI) has been regarded as an efficient and cost-saving method to improve the flexibility of the energy systems. However, the acclaimed benefits in most studies are found in specific cases with traditional middle-temperature systems. The cases where DHNI is not feasible are unclear and the applicability of DHNI in future low-temperature district heating (LTDH) systems requires further investigations. Therefore, this study applied a top-down methodology where the practical storage potentials of DH networks are evaluated based on field investigations of 134 Swedish DH networks and 25 Chinese DH networks with various sizes and demand densities. Empirical relationships between the heat density and storage potentials are established and analyzed. Then, bottom-level analysis from technical and economical aspects are conducted on a variety of application scenarios for DHNI, including different temperature levels, heat sources, control strategies and renewable energy profiles. It is found that in LTDH system, by raising the network temperatures to actively use the DHNI, the heat source efficiency is reduced regardless the size and density of the network and, thereby, making the DHNI infeasible. This implies that the DHNI is only applicable in middle-temperature systems with combined heat and power plant (CHP) as a heat source in the extraction mode. Furthermore, the back-pressure mode is not economically attractive. In summary, the results from a multi-scenario analysis identified limited benefits of the DHNI, implying a proper consideration of its roles in future works.

1. Introduction

To reach the target of carbon neutral society and 100% sustainable future, accelerating growth of renewable energy is predicted in most countries and a large share of it, such as the wind and solar power, has intermittent and variable characteristics [1,2]. The efficient integration of these variable renewable energy (VRE) sources, while keeping secured energy supplies and acceptable economic expenditures, is a major issue in the future energy system [3].

The integration of VRE in the electricity sector demands an increased flexibility, which could be provided by thermal energy storage (TES) technologies in heating systems in an efficient and cost-effective manner [4–6]. Currently, the heating demand in the residential sector accounts for 17% of Europe's final energy consumption [7] and is expected to remain so for the forecasted future. With the use of power-to-heat technologies such as the heat pump and the combined heat and power (CHP) plant, the integrations of VRE can be improved through the flexible management of heating load [8,9]. In recent years, various types of TES technologies have been applied in district heating (DH) systems,

with the aims of shifting the load, improving the heat source efficiency and reducing the operation cost [10]. Recent applications of the TES technologies can be found in a review by Guelpa and Verda [11].

To deal with the variability and uncertainty of VRE within a short period like one day, growing interests are found in utilizing the storage potentials of the district heating network inertia (DHNI) [12]. By actively increasing the temperature levels of the circulation water inside the supply pipes, additional flexibilities can be provided by the network with no extra investment. Meanwhile, the heat losses from pipes are slightly increased [13]. Commonly, the supply water temperature increase is limited to several degrees, such as 10 K or 15 K. The storage capacity of the return pipes can be also used if the temperature increase in the return pipes is allowed. Compared to the standalone TES technology such as the central heat accumulation tank, the use of DHNI is easily implemented [13]. Thus, the importance and potentials of the DHNI are gradually identified in recent studies. Lund [14,15] estimated the overall storage potentials of the Danish DH networks as 5 GWh, which is approximately 4.3% of the average daily DH load, based on the assumption of a 10 K temperature increase. Zheng et al. [16] evaluated the network storage capacities in Northern China and calculated the

^{*} Corresponding author.

E-mail address: yichi@chalmers.se (Y. Zhang).

<https://doi.org/10.1016/j.applthermaleng.2022.118813>

Received 25 November 2021; Received in revised form 5 April 2022; Accepted 7 June 2022

Available online 11 June 2022

1359-4311/© 2022 The Authors. Published by Elsevier Ltd. This is an open access article under the CC BY license (<http://creativecommons.org/licenses/by/4.0/>).

Nomenclature		Cost	Cost
<i>Abbreviations</i>		F	Fuel consumption rate (MW)
BP	Back-pressure	η	Efficiency (%)
CHP	Combined heat and power	P	Electric power (MW)
CNY	Chinese Yuan	Pr	Price (CNY/kWh)
COP	Coefficient of performance	Q	Heating power (MW)
DH	District heating	T	Temperature ($^{\circ}\text{C}$ or K)
DHNI	District heating network inertia	θ	Proportion (%)
ECR	Effective conversion ratio	<i>Subscripts</i>	
LTDH	Low-temperature district heating	ch	Charge
MTDH	Middle-temperature district heating	dch	Discharge
SOC	State-of-charge	el	Electricity
TES	Thermal energy storage	$grid$	National electric grid
<i>Symbols</i>		$h2p$	Heat to power
α	Combination factor	τ	Time step

reduced wind power curtailment. Since the study is based on provincial statistics, it was concluded that the results could not be scaled down to reflect the practical conditions. Fredriksen and Werner [17] described a limited storage capacity of less than 5% of the maximum heating demand for DHNI in Sweden.

While the above-mentioned studies have theoretically analyzed the storage potentials of DHNI, several case studies were conducted in recent years to investigate the practical benefits of the DHNI, especially the improved integrations of VRE. The cases studies were mostly located in Northern China [18–23] and Scandinavian countries [24–28], where high shares of building heating demand are supplied by DH. Zheng et al. [18] developed an integrated heat and power dispatch model and optimized the network temperatures to actively use the storage capacity for wind power integrations, based on a case study of a real DH system with CHP plant in China. Using the same model, the storage utilization strategy was compared to other solutions such as the exhaust heat recycling, in terms of the total primary energy consumption [19]. Similar modelling methodologies were found in [21] where the DHNI was studied in combination with the inertia of the building thermal mass. Improved VRE integrations of up to 10% were found in a case DH system with CHP plant and wind power in Northern China [23]. In case of European cities such as Helsinki, with an average daily heating demand of 17–20 GWh, the storage potential of DHNI was estimated as 1.5 GWh [24,25]. It was further proved that for a certain scheme, all the surplus VRE production could be absorbed by the power-to-heat technologies with TES. However, the coefficient of performance (COP) of the heat pumps (HPs) were assumed as constant, which is not true when raising the network temperatures for active storage.

The above-mentioned studies quantified the benefits from the DHNI in cases where a combination of DH and certain heat sources provide feasible conditions for this technology. Due to the different boundary conditions that were considered, the results vary between cases and the preferable application scenarios of the DHNI are still unclear. Since the network temperatures are actively increased, both the efficiencies of heat sources and the associated operational issues such as heat losses are inevitably influenced. However, the resulting consequence was not investigated in most of the cited studies [18–23,26–28], possibly because all considered traditional middle and high temperature DH systems with CHP plants as the main heat source. These cases are also referred to as the third generation DH [29], where the supply and return water temperatures are around 100 $^{\circ}\text{C}$ and 50 $^{\circ}\text{C}$, respectively. The supply water is heated by the steam with a much higher temperature, extracted from the CHP plant. Therefore, actively raising the network temperature has little impact on the source efficiency. Other studies have assumed constant heat source efficiency when utilizing the

network inertia [24,25]. However, this is not appropriate for heat sources whose efficiencies are associated with the supply water temperature [30]. Indeed, the additional costs associated with the increased temperatures might be larger than the proposed benefits.

Unlike the traditional systems, the low-temperature district heating (LTDH) system has been recognized as a key DH configuration in the future [29]. In such system, associated with the lower heating demand in the future, the supply and return water temperatures are reduced to around 55 $^{\circ}\text{C}$ and 25 $^{\circ}\text{C}$, respectively. Major measures to achieve the low-temperature target from the space heating system, domestic hot water system, intelligent control system were investigated and summarized in previous works [5,29]. In consequence, key benefits including better utilization of low-temperature waste heat and integration of renewable energy sources, as well as lower losses in transportation networks, are enabled. However, heat sources such as HPs and the acknowledged benefits are sensitive to the temperature changes in the network. Considering these changes, whether the use of DHNI is still applicable in the LTDH systems, has not been clearly proven.

In addition to the network temperatures and the heating sources, the benefits of DHNI are also influenced by various variables. It should be noted that the results of the above-mentioned studies are only limited to certain VRE surplus conditions. As the balance between the VRE supply and the energy demand changes, the benefit of the DHNI also changes. Besides, as pointed out in [13,23], the control strategies for the flowrate and the return water temperatures have significant influences on the usable storage capacity and load shifting benefits. Although the different operation modes were compared in [23], the focus was more on the operational cost such as the pumping cost, while the influences on the heat source efficiency and storage capacity were less covered. With these questions unsolved, the proposed potentials and benefits of the DHNI might be over-exaggerated.

According to the above literature review, limitations and challenges exist for the use of the DHNI. Because the single case applications were reported in the previous studies, the application ranges of the DHNI are limited. To support the development of a sustainable energy system in the future, more comprehensive understandings of the DHNI are much needed. Therefore, this paper aims to answer the questions of where and why the use of DHNI is feasible. The study is based on a purposely-developed multi-scenarios analysis with the considerations of the technical and economical perspectives on the system level. The focus is how the system performance is influenced by different operation conditions, including the temperature levels, types of heat sources, control strategies and the VRE balances. Considering the currently large share of DH in the building stock, various DH networks in Sweden and China with different sizes and densities are investigated. The range of storage

potentials from the network inertia is also specified and compared in terms of countries. According to the findings from the multi-scenario analysis, the key performance indicators of the DHNI are summarized, which can be used to identify the feasibility of the DHNI at an early design stage. Finally, implications for the applications of the DHNI in future energy systems are provided.

2. Methodology

The investigations of the storage potentials of the practical DH networks are based on 134 Swedish cases and 25 Chinese cases, as explained in Section 3. These cases cover a wide range of sizes and heating demand densities, i.e. from 1 GJ/m to 200 GJ/m, to understand their influence on storage potential. The share of storage potential in the heating demand is also revealed. Among the studied DH systems, a city-scale DH system is selected as the reference case for bottom-level multi-scenarios analysis. The integrated DH model to simulate the dynamic performance of the DH system is based on a previous work by the authors [31]. To account for DHNI, the earlier DH model is upgraded with two new representations, a numerical model of the network inertia and a dispatch model of heat sources, as explained in this section. The use of the DHNI under multi-scenarios is simulated and the results are shown in Section 4.

2.1. Case description

The reference case for the multi-scenarios analysis comprises a DH system in a town with approximately 50,000 inhabitants [32], located in the Hebei province in Northern China. The town belongs to the cold climate zone with an average temperature of -4.6°C in January of the typical meteorology year. This town is chosen because it represents a vast number of middle-sized towns in China. For smaller DH systems such as those in the rural communities, the storage potentials of the networks can be as small as 0.5% of the daily heating demand, as pointed out in [17] as well as in the hereafter analysis in Section 3. As for larger DH systems in major cities, more complex networks with multiple heat sources are often built, which have complicated hydronic conditions that are difficult to be modelled. Therefore, they are neglected in this study.

The total heated floor area by the main-case DH is 4.48 million m^2 , comprising residential, commercial, and industrial areas. The end-use buildings are grouped into 71 substations, as shown in Fig. 1. Each substation has heat exchangers that separate the secondary network from the primary one. To simplify the modelling process, the end-users connected to the same substation are aggregated into one representative end-user, on which the modelling of the buildings and the secondary networks is conducted. This simplification is acceptable since the end-users connected to one substation often include buildings with similar thermal properties and load profiles. Correspondingly, the secondary network is represented by a pipe with certain length. In this study, the thermal inertia of the primary network is considered. The total length of the primary networks in the main-case DH is 52.3 km and the detailed lengths of each pipe diameter are shown in Table 1. As a result, the total volume of the circulating water inside the two-way pipes is 25,160 m^3 . Considering a typical temperature increase of 10 K that was used in previous studies [18,19], the storage capacity of the primary pipes is 294 MWh.

The thermal properties of the end-use buildings are derived from the local housing department and are then used as known input parameters in the building models. In general, the heated buildings can be classified into three energy-efficient types, according to the building energy standards in Northern China [33–35]. The total heated floor area and average heat consumption at the building level of each type is shown in Table 2, based on the historical operation data from the local district heating company during the heating period from 2018 to 2019.

The investigated scenarios in this study are summarized in Table 3.

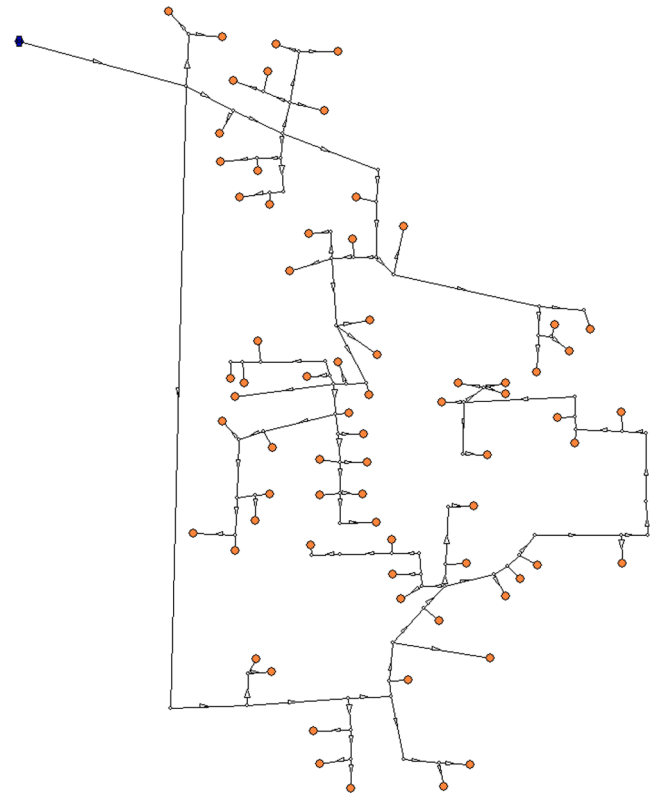


Fig. 1. Network layout of the case DH system.

Table 1

Pipe diameters and total one-way lengths of the primary network based on [32]

Pipes	Length (m)	Volume (m^3)
DN125	24	0.3
DN150	3,820	67
DN200	6,329	199
DN250	7,047	346
DN300	4,144	293
DN350	5,371	516
DN400	4,023	505
DN450	864	137
DN500	1,852	363
DN600	7,597	2,147
DN700	600	231
DN800	1,300	653
DN900	1,324	842
DN1000	8,000	6,280
Total	52,295	12,580

Table 2

Building types, accumulated heat consumptions and heating power demands at the building level during the heating period of 2018–2019.

Types	Floor area (m^2)	Heating energy demand (kWh/m^2)	Heating power demand (W/m^2)	Ref
Non-energy-efficient building	1,696,318	140	58.3	–
Second-level energy efficient building	2,169,586	98	46.6	JGJ 26-95 [34]
Third-level energy efficient building	612,861	75	40.1	JGJ 26-2010 [35]

Table 3

Summary of the investigated systems and scenarios.

Systems	Heat sources	Control strategies	VRE supply and electricity demand
MTDH	Extraction CHP, back-pressure CHP	Fixed flowrate, variable flowrate	VRE: 300 MW to 700 MW
LTDH	Back-pressure CHP, large-scale HP		Demand: 50% and 100%

The traditional middle-temperature district heating (MTDH) system has design supply and return water temperatures of 90 °C and 50 °C, respectively, and is the current operating system in the case town. In contrary, the LTDH represents a possible scenario in the future, with lower supply and return water temperatures of 55 °C and 25 °C, respectively. Since the focus of this study is on the DHNI, the feasibility of the LTDH system is not considered. Indeed, comprehensive investigations and evaluations are needed when planning for the LTDH system, as pointed out in [29]. Correspondingly, several heat sources options, located at the central heating plant in the Northwest part of the town, are available as investigated scenarios. The specific parameters and models of the heat sources are explained in Section 2.3 in detail.

To investigate the application ranges of the DHNI, several scenarios with different VRE supply and electricity demand profiles are modelled, as presented in Table 4 and Table 5. Among the available VRE, wind power is chosen because it is developing fast in Northern China but also facing serious curtailment issues [36]. In the baseline scenario, the installed capacity of wind power is 500 MW and this scenario is also named VRE500, accordingly. Based on the actual power generating profiles in Northern China [18], the annual wind power production is 1.4 TWh, equivalent to 2801 full-load hours. In the 100% electricity demand scenario, the demand of the case town and the surrounding villages is considered, summing up to 1.8 TWh each year. The demand profile is derived from the actual profile in Jilin province [18], as shown in Fig. 2.

The studied town is currently having higher energy intensity than the average level of towns in China. With the national target towards carbon peak and carbon neutrality [37], the energy-consuming industries in the case town are planned to be phased out and replaced with higher efficiency industry. However, there is no specific plan or quantitative target for the electricity demand in the future. The 50% electricity demand scenario is assumed as one possible energy-saving condition in the future.

In addition to the heat supply service, the district energy company is also supplying electricity to the case town, with on-site CHP plant, wind power, or electricity from the national grid. Therefore, the main objective of using the DHNI is to minimize the operational cost for the local district energy company by increasing the wind power share. The objective function and related energy costs are introduced in Section 2.2.

2.2. DH system models

Aforementioned model of the integrated DH system developed by the authors [31] is used in this study. The general modelling methodologies are thus only briefly explained in this section, while the detailed

Table 4

Installed capacities and annual power generations for five VRE scenarios.

Scenarios	Installed capacity(MW)	Annual generation(GWh)
VRE300	300	840
VRE400	400	1,121
VRE500 ¹	500	1,401
VRE600	600	1,681
VRE700	700	1,961

¹ Baseline scenario.**Table 5**

The maximum power and annual demand for the two household electric demand scenarios.

Scenarios	Maximum power(MW)	Annual demand(GWh)
100% electric demand ¹	228.6	1,800
50% electric demand	114.3	900

¹ Baseline scenario.

modelling principles, variables and functions can be found in [31]. As shown in Fig. 3, the model has four main steps. In the first step, based on the input building properties and the weather data, the demand profiles for space-heating are calculated by a lumped capacitance building model with five resistances (5R1C), according to EN ISO 13,790 [38]. Domestic hot water draw-off profiles are generated by stochastic modelling tool called *DHWcalc* [39]. Then, the compartments in the DH systems, such as the heat sources, substations and circulating pipes, are designed in the second step. In the third step, the temperatures and flow dynamics of the networks are modelled by the node method [40,41], with considerations of the transport delay and heat loss. This scenario is also named the reference (REF) scenario, where the active load management is not implemented. Then, in the fourth step, the active usage of the DHNI is optimized. The multi-scenarios analysis is conducted on this model, by changing parameters according to specific designs in scenarios.

Because the target of the optimization process is to find the minimum operating cost, four major parts of the operating cost are considered, which are the fuel cost of the heat source, the electricity cost from the grid, the electricity sold back to the grid, and the cost for water circulating pumps, as written in Eq. (1). The costs associated with the auxiliary equipment are neglected because they only have small shares in the total cost. The selling price of electricity from the CHP plant is set the same as the buying price from the grid. For wind power, the selling price differs a lot with policies and subsidies. In this study, to focus on the local integration of renewable energy, which is the core idea of future smart energy systems, the market price of surplus wind power is set as zero.

$$\min Cost = \sum_{\tau} (Pr_{fuel} \bullet F_{HS,\tau} + Pr_{el,grid} \bullet (P_{el,grid,\tau} + P_{pump,\tau}) - Pr_{el,grid} \bullet P_{el,sold,\tau}) \quad (1)$$

where $P_{el,grid,\tau}$ is the amount of electricity bought from the grid at time τ and price $Pr_{el,grid}$. The latter is set to 0.6 Chinese Yuan (CNY)/kWh, according to the average electricity price on the market. For the whole year of 2020, one Chinese Yuan (CNY) equals to 0.145 US dollar on average. $F_{HS,\tau}$ is the fuel consumption of the heat source at time τ and Pr_{fuel} is the fuel price. As for the CHP plant, the biomass fuel which is briquette from crop straw and wood, with an average calorific value of 16 MJ/kg is used. According to the local market, the biomass price is 660 CNY/t, which corresponds to approximately 0.15 CNY/kWh. Finally, the electricity price for the heat pump is set the same as the price from the grid.

To integrate more wind power and to reduce the electricity from the grid, the electric load is changed by adjusting the heating load through the active use of the network inertia. In practice, the water temperatures at the heat source are actively controlled, i.e. increased or decreased, and the difference to the designed water temperature implies charging or discharging heat in the network. According to the literature on safety operation of the DH pipes [12], the temperature increase speed of 1 °C/hour is considered, corresponding to the maximum charging or discharging power of 14.7 MW for using the network inertia.

For each time step τ , both the heating and electricity demand shall be fulfilled, as written in constraint functions in Eqs. (2) and (3).

$$Q_{HS,\tau} \geq Q_{demand,\tau} \quad (2)$$

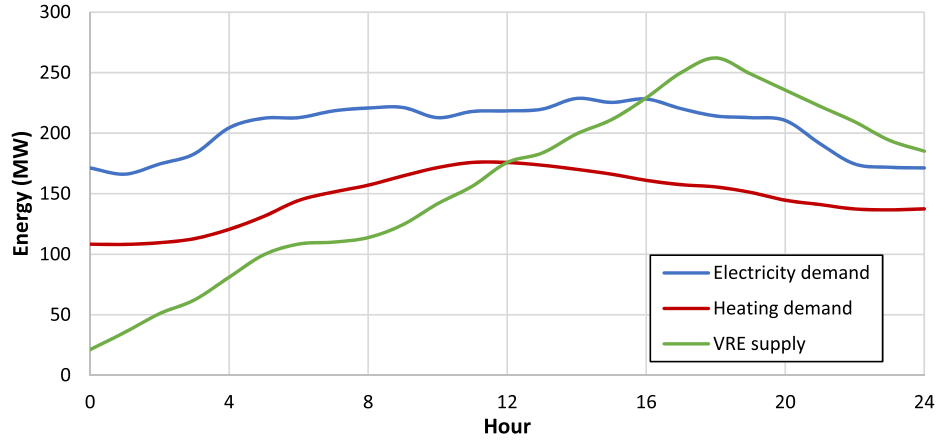


Fig. 2. Heating demand, electricity demand, and VRE supply profiles of the baseline scenario on the typical heating day, found on Jan 2nd.

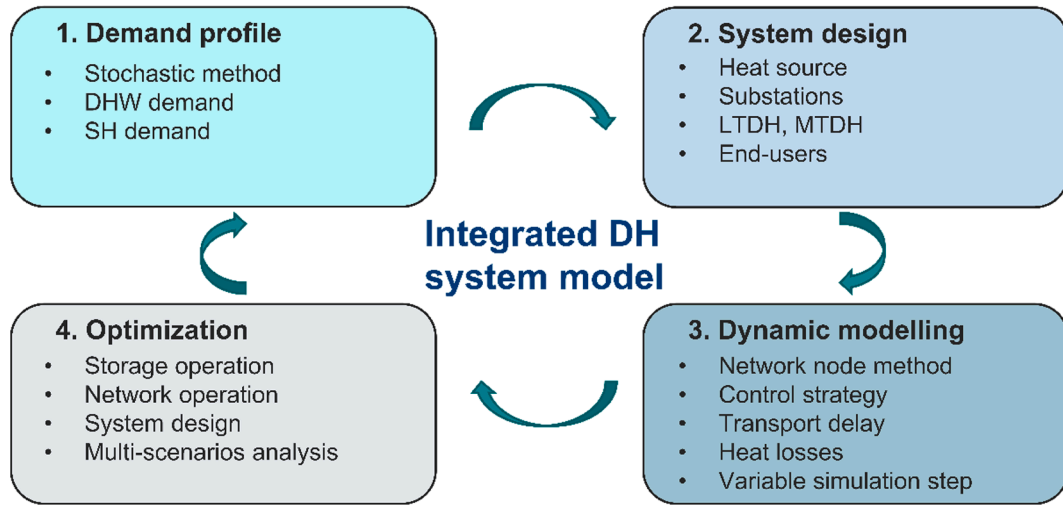


Fig. 3. Schematic of the main steps of the integrated DH system model.

$$P_{el,CHP,\tau} + P_{el,grid,\tau} + P_{VRE,use,\tau} \geq P_{el,demand,\tau} \quad (3)$$

where $Q_{HS,\tau}$ and $Q_{demand,\tau}$ are the heat supply and demand at time τ , respectively. $P_{el,CHP,\tau}$ is the electricity generated from the CHP plant, $P_{VRE,use,\tau}$ is the integrated wind power while $P_{el,demand,\tau}$ is the electricity demand. If the heat source is an electricity consumer, like the HP, the related demand is added to the right-hand side of Eq. (3).

Due to the non-linear characteristics of the complex networks, a combined central optimization and local control strategy is applied in this study, as shown in Fig. 4. In this way the optimization process is

simplified while maintaining realistic characteristics of the DH system.

The whole model is developed and performed in MATLAB. The dynamic calculation step is set as one minute in accordance with the demand profile, and the optimization time step is set as one hour. The length of an optimization cycle is set as 5 days, considering the accuracy of forecast and the control complexity.

Two control strategies for the flowrate are considered to utilize the network inertia, as shown in Table 3. Under the variable flowrate strategy, only the supply water temperature is adjusted while the return water temperature is controlled within an acceptable small range to assure the heat source efficiency. In this way, only half of the storage

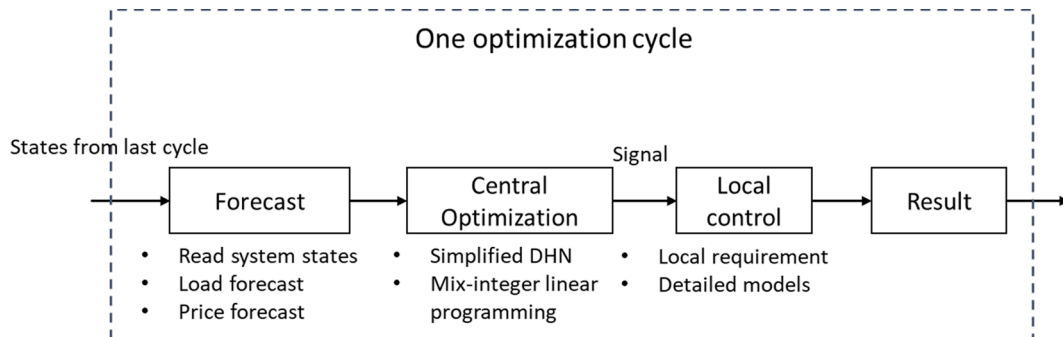


Fig. 4. Schematic diagram of the combined central optimization and local control strategy, from [31].

potential of the network is used, as indicated in previous works [13,23]. Besides, the flowrate is reduced when raising the network temperature, which further hampers the storage potential. Instead, the “fixed flowrate, variable temperatures” control strategy in both the supply and return lines is proposed to better utilize the network inertia. Due to the transportation delay in large DH networks, the fixed flowrate control strategy is commonly applied in systems with less frequent demand changes. Such DH systems are prevailing in China, covering typically only the space heating demand while the domestic hot water is produced locally, by domestic gas boilers or electric heaters. The temperatures of the network are decided by the forecasted load condition, which is usually based on the weather profiles in practical systems [42].

The performance of the network inertia under different flow strategies, i.e. for both the variable and constant flows, are presented in Section 4.1–4.2. The comparison between the two strategies is discussed in Section 4.3. The pumping power is calculated according to the hourly flowrate and the network pressure drop. The economically feasible pressure drop of 50 Pa/m and the pump efficiency of 70% are assumed in the calculations.

2.3. Heat source models

Since the focus of this study is to investigate the improved VRE integrations achieved by the DHNI, the heat sources that connect the heating and electricity sectors are chosen, including the CHP plants and HPs, as shown in Table 3. It should be noted that the use of the storage unit can also bring in benefits from other aspects, such as the peak load shaving and the reduction of ramping costs of the heat sources [10,11]. These aspects are currently omitted in this study.

Two types of CHP plants are considered, which are the extraction plant and the back-pressure plant. As for the extraction plant, the middle pressure steam with the temperature of approximately 150 °C is extracted from the steam turbines to heat the circulating water. Therefore, the active use of the network inertia is simply considered to have no influence on the source efficiency. The heating and electricity output can be adjusted by the amount of extracted steam, within certain minimum and maximum limits. Meanwhile, the main steam flowrate can be adjusted by changing the boiler load. For the analysis, an extraction plant with the nominal power generating capacity of 250 MW is selected with a feasible operation range as shown in Fig. 5. Any operating point within this range can be expressed by the convex combination of the coordinates of the corner points [18,43], using the Eqs. (4)–(6). It

should be noted that there are various methods to improve the efficiency of the CHP plant [44]. These methods are not considered for the analysis but are discussed in Section 5.

$$Q_{CHP,\tau} = \sum_{N=1}^4 (\alpha_{N,\tau} \bullet Q_{CHP,N}) \quad (4)$$

$$P_{el,CHP,\tau} = \sum_{N=1}^4 (\alpha_{N,\tau} \bullet P_{CHP,N}) \quad (5)$$

$$F_{el,CHP,\tau} = \sum_{N=1}^4 (\alpha_{N,\tau} \bullet F_{CHP,N}) \quad (6)$$

where $\alpha_{N,\tau}$ are the combination factors of four corners, complying with the constraints written in Eq. (7). The maximum ramping rate of the main boiler is set as 30%/hour, taken from the design brochure of the CHP plant. The boiler efficiency is assumed as 90% to calculate the primary energy consumption.

$$\sum_{N=1}^4 \alpha_N = 1 \quad (7)$$

As for the back-pressure CHP plant, the only adjustable option is the boiler load. Thus, the plant has fixed power-to-heat ratio and the feasible operation range is a straight line on Fig. 5, e.g. line C-B. The parameters of the chosen back-pressure plant for the MTDH scenarios are shown in Table 6. The circulating water is heated by the low-pressure exhaust steam from the turbine. As the required supply water temperature increases, the exhaust steam pressure and temperature shall also be increased. Correspondingly, the electric power and heating power are changed, as shown in Table 6. As is explained in Section 4, this change has important influences on the wind power integrations and the benefits of the DHNI.

Table 6
Parameters of the back-pressure CHP plant for MTDH scenarios.

Load	Exhaust temperature (°C)	Main steam (t/h)	Electric Power (MW)	Heating power (MW)
Max	100	500	87.8	336.7
Min		150	26.3	101.0
Max	110	500	86.0	338.9
Min		150	25.8	101.7

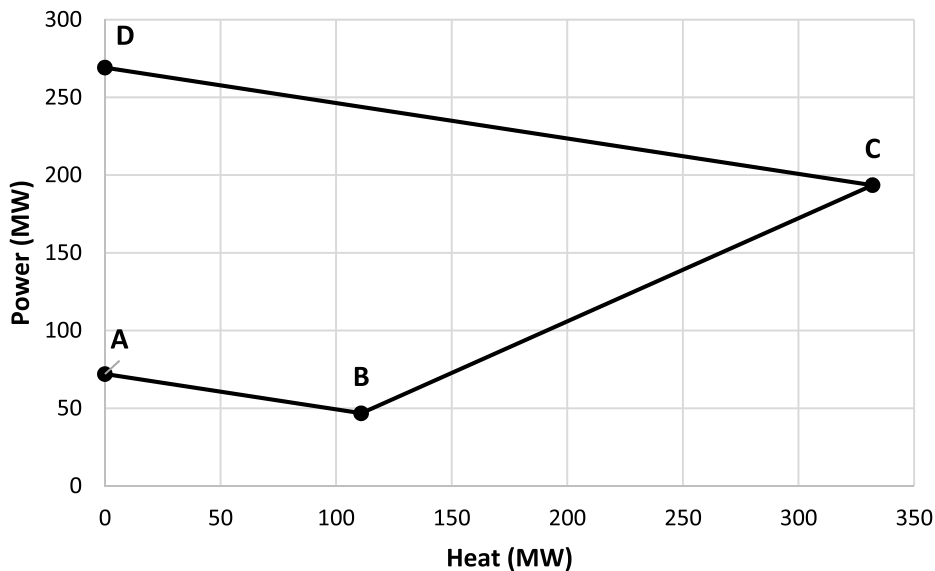


Fig. 5. Feasible operation range of the extraction CHP plant.

Due to its low efficiency for high-temperature applications, the HP is only used in the LTDH system, with a nominal supply water temperature of 55 °C. The design parameters of the chosen waste water source heat pump are presented in Table 7. The practical COP is calculated by the empirical equation with the condensing temperature T_C , evaporating temperature T_E , and the thermodynamic efficiency of 0.65 [45], as written in Eq. (8). The waste water at the source side is considered to have a stable temperature of 15 °C.

$$COP = 0.65 \cdot \frac{T_C}{T_C - T_E} \quad (8)$$

2.4. Key performance indicators

The state-of-charge (SOC), which is storage level of the network inertia, is calculated based on the instantaneous network branch temperature $T_{b,\tau}$ from the system model, as written in Eq. (9).

$$SOC_\tau = \sum_b C_b \cdot (T_{b,\tau} - T_{b,design}) \quad (9)$$

where $T_{b,design}$ is the design temperature of branch b . C_b is the storage capacity of the branch pipe, calculated from the flow rate and the heat capacity of water.

To compare the storage performance of the network inertia under various scenarios, the number of full-load discharge cycles is defined in Eq. (10).

$$Full-load \ discharge \ cycles = \frac{\sum_\tau Q_{dch,\tau}}{SOC_{design}} \quad (10)$$

where the $Q_{dch,\tau}$ is the discharged energy at time step τ . SOC_{design} is the designed state-of-charge, which is quantified to 147 MWh if only the supply pipes are used for storage.

To evaluate the performance of improved VRE integrations, the effective conversion ratio (ECR) of the storage unit, which explains the effective usage of the discharged energy, is defined in Eq. (11).

$$ECR = \frac{\sum_\tau P_{VRE,use,\tau}}{\sum_\tau Q_{dch,\tau}} \quad (11)$$

During the entire year of 2019, the dynamic performance of the reference system without active storage usage are firstly investigated. Then, the case DH systems with the use of the network inertia under different scenarios are modelled and compared. The improved VRE integration rate is calculated to evaluate the benefits of the DHNI, as defined in Eq. (12).

$$ImprovedVREintegrationrate = \frac{\Delta \sum_\tau P_{VRE,use,\tau} - \Delta \sum_\tau P_{VRE,use,ref,\tau}}{\sum_\tau P_{VRE,\tau}} \quad (12)$$

where the $P_{VRE,\tau}$ is the wind power production at time step τ .

3. Storage potentials

In this section, the storage potentials of the networks in Swedish DH systems and Chinese DH systems are evaluated and compared. The information about the Swedish DH systems is derived from the previous investigation of 134 DH systems [17]. Based on that, the average pipe diameters were estimated through linear heat density Q_s/L , as written in Eq. (13), from [46].

$$d_a = 0.0486 \cdot \ln\left(\frac{Q_s}{L}\right) + 0.0007 \quad (13)$$

Then, the storage capacities of the networks are estimated at different temperature increase scenarios. The ratio of the storage capacity in the daily heating demand is calculated and shown in Fig. 6, assuming on average 180 heating days in the Swedish DH systems. It should be noted that only the supply pipes are considered in the estimations. As can be seen, the ratio of storage capacity increases up to approximately 6 GJ/m and then decreases as the linear heat density becomes larger. Even for a high temperature increase of 20 K in the most favorable scenario, the storage capacity in the investigated DH networks is only 1.6 % of the daily heating demand. In the 10 K temperature increase scenario, the storage capacity is always less than 0.8% of the daily heating demand.

To enlarge the studied linear heat density range, investigations were conducted about the network information and heating demand of 25 DH systems in China. These Chinese systems are located in a wide range of areas from towns to metropolitans, which have larger heat density and larger numbers of end-users. The linear heat densities and average pipe diameters are summarized in Fig. 7. Instead of the specific correlation equation like Eq. (13), a general tendency of larger network capacity in higher demand area is utilized to find the average pipe diameter as summarized in Fig. 8. Compared to Swedish DH systems, under the same heat density, the average pipe diameter in Chinese DH systems is much larger. This is explained by two reasons:

- 1) The pipes are designed for the DH systems and heating loads in the future, accompanying the rapid urban development in China. Thereby, the main transportation pipes are oversized compared to the current demand level.
- 2) The sizing of the DH networks in Europe is done with the design pressure drop of 200 Pa/m, while in China this number is lower, around 50 Pa/m. This fact leads to much bigger pipe diameters in China than in Europe.

Correspondingly, the storage capacities of the supply pipes in these DH systems are calculated and summarized in Fig. 8. For each temperature increase case (10 K or 20 K), the length of the heating period is investigated and used for calculating the average daily heating demand. The latter is further used for analyzing the share of storage capacity in the demand.

Similar as the Swedish DH systems, the ratio of the storage capacity firstly increases and then decreases in larger systems. Considering the temperature increase of 10 K, the storage capacity of the networks is on average 4 % of the daily heating demand. The results on real DH systems have identified the limited potential of network storage, which is further used in the theoretical analysis of the storage benefits in Section 4.5.

4. Multi-scenario analysis results

Based on the above-mentioned methodologies, the case DH systems and the scenarios explained in Section 2 are simulated for an annual operation period. The performance of the network inertia under different network temperature levels, heat sources, flowrate control strategies and the VRE balances, are compared and discussed in this section.

4.1. MTDH scenarios

By comparing the MTDH systems with and without the active use of the network inertia, the performance and benefits of the network inertia are explained. Taking the system with the extraction plant as an example, the hourly heat supply and SOC of the network inertia during five winter typical days, from the Jan 1st to the Jan 5th, when there are

Table 7

Parameters of the HP for LTDH scenarios.

Name	Capacity (MW)	Outlet T (°C)	Thermodynamic efficiency	Design COP
Waste water source heat pump	350	55	0.65	4.8

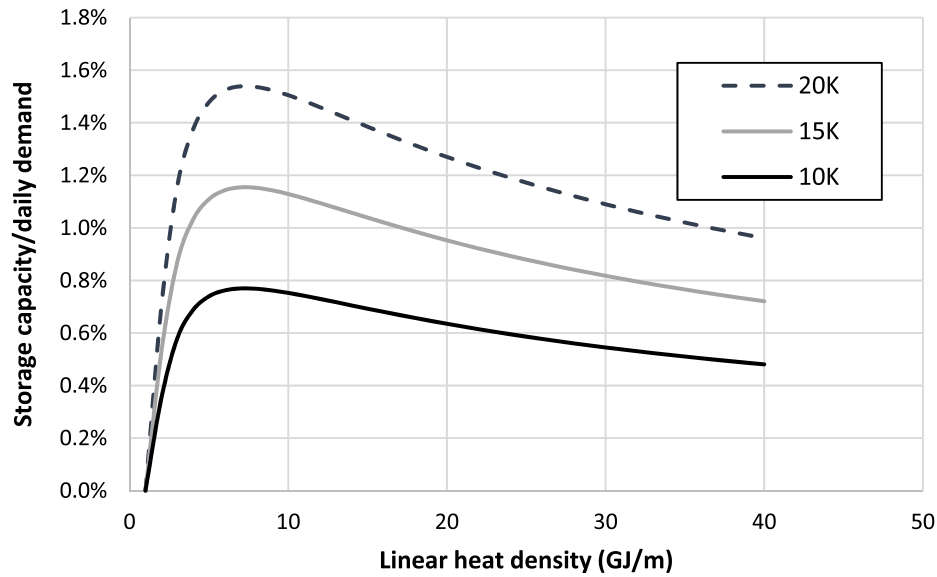


Fig. 6. The ratio of the storage capacity in the daily heating demand in Swedish DH systems.

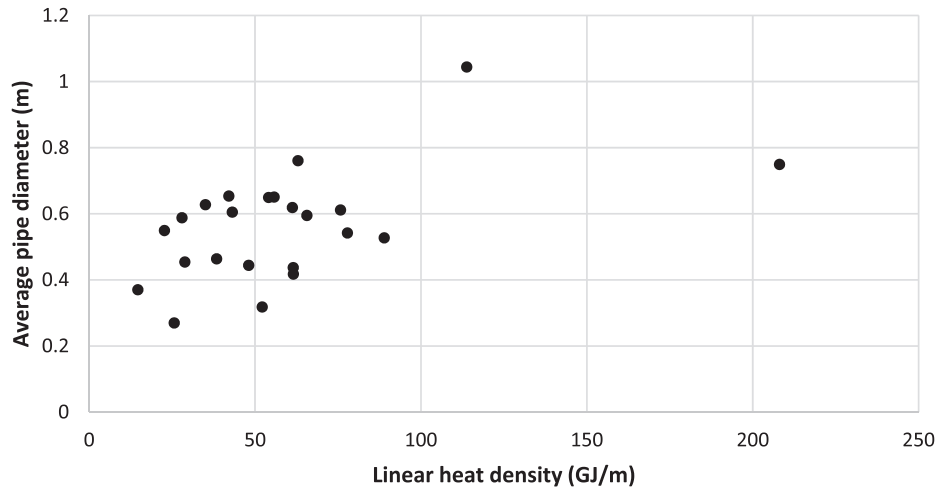


Fig. 7. The relationship between the average pipe diameter and linear heat density.

variations in both the electricity production of the CHP plant is reduced to as much as possible to integrate the surplus VRE. Since the heat and power output are connected, the heating production is also influenced, as shown by the orange curve in Fig. 9. Then, the stored heat inside the network is used to fulfill the heating demand, e.g. from 8 am to 6 pm of Jan 1st, as shown by the difference between two curves in Fig. 9. In consequence, the synergy between heating and electricity is achieved and the VRE integration is improved, as shown in Fig. 10. The hourly supply and return water temperatures are presented in Fig. 11 to explain how the storage capacity is utilized. For example, in the period from 8 am to 6 pm of Jan 1st where the stored heat is discharged, the network supply water temperature is reduced from 100 °C to 90 °C while the end-use heating demand is still fulfilled. The charged and discharged heat is expressed by the temperature rise and fall in Fig. 11, respectively. Since the variable flow rate strategy is applied, the return water temperatures are kept at a relatively stable range, while the supply water temperatures are adjusted.

In the reference MTDH system, the annual total heat supply is 578.1 GWh, of which 27.7 GWh is the heat loss through pipes. In the system with active DHNI usage, although the water temperature level is increased, the circulating flowrate is reduced in the meanwhile. Thus,

the total heat loss is only slightly increased to 28.6 GWh.

Similar modelling methodologies are applied for the MTDH system with the back-pressure plant as the heat source. The annual electricity supply and demand for the investigated systems are summarized in Fig. 12. The demand is constituted of the direct use of CHP power, integrated VRE and the electricity bought from the grid. By actively using the DHNI, the integrations of the VRE are improved by 6 GWh and 4.3 GWh respectively, in extraction and back-pressure systems. However, due to the restricted storage capacity, the increased VRE usage is only approximately 0.4% of the total VRE supply and 0.3% of the total electricity demand.

To evaluate the storage performance, the effective conversion ratio (ECR) of the storage unit, explained in Section 2.4, is calculated for the case systems. As shown in Table 8, in the extraction plant scenario, only around 31% of the discharged energy is effectively used to shift the electric load. This can be mainly explained by two reasons. First, the average heat-to-power ratio of the extraction CHP plant is around 2, which is the baseline conversion factor between the heat and power sectors. Second, due to the diverse heating demand and the local control strategies, the practical control of the discharging process deviates from the ideally optimized process and, therefore, limits the storage benefits.

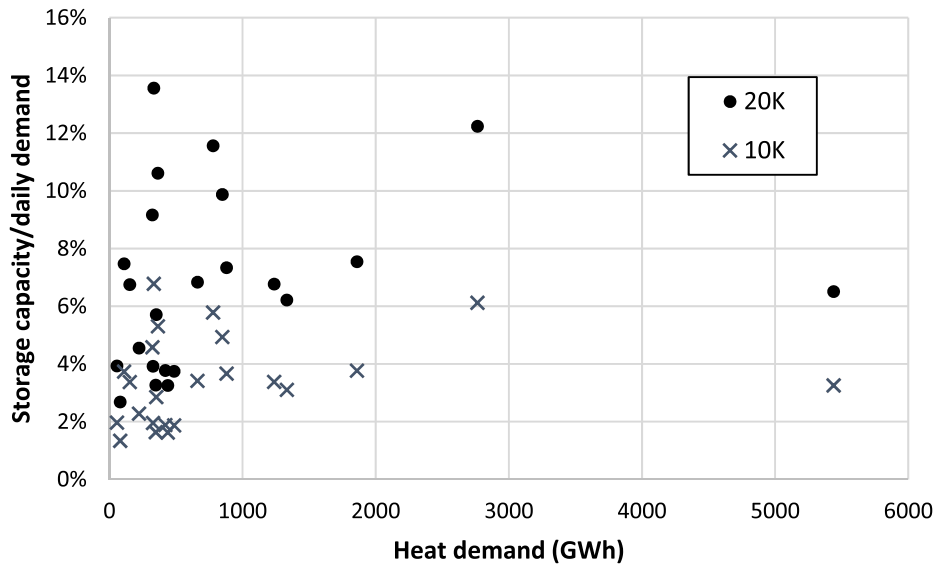


Fig. 8. The ratio of the storage capacity in the daily heating demand in Chinese DH systems.

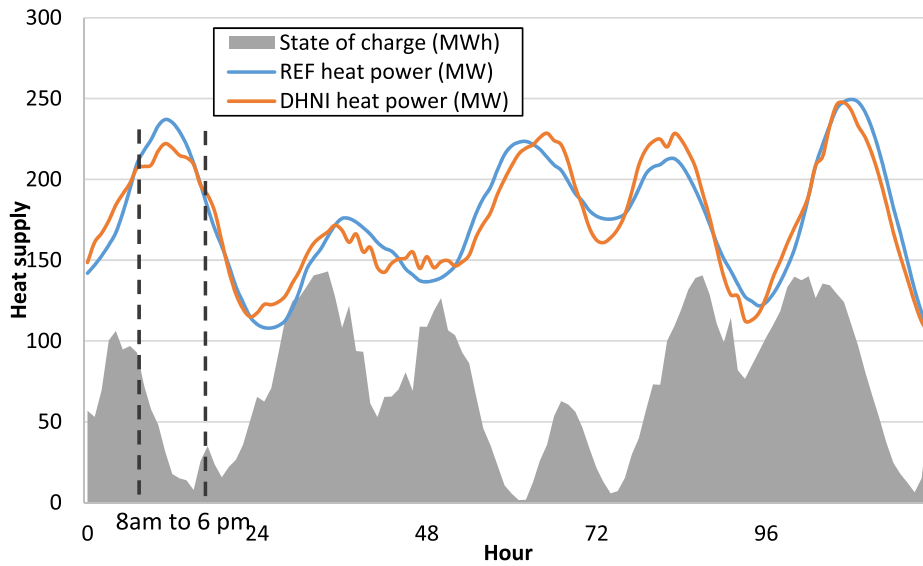


Fig. 9. Hourly heat supply and storage state-of-charge for five typical days from Jan 1st to Jan 5th.

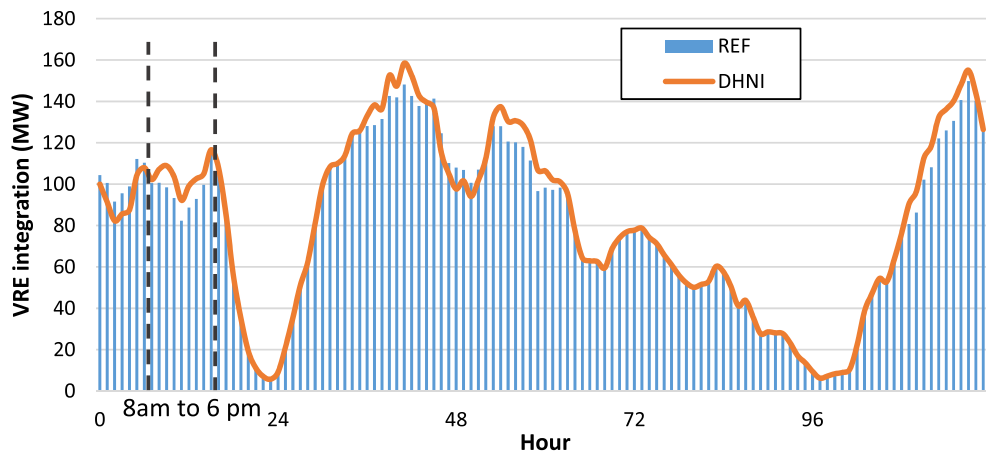


Fig. 10. Hourly VRE integrations of the REF and DHNI systems for five typical days from Jan 1st to Jan 5th.

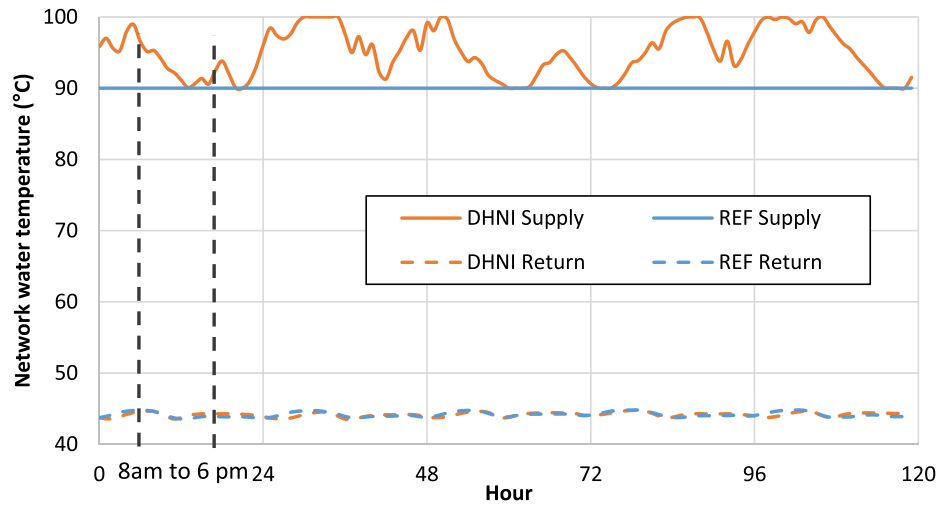


Fig. 11. Network supply and return water temperatures of the REF and CHP systems on five typical days from Jan 1st to Jan 5th.

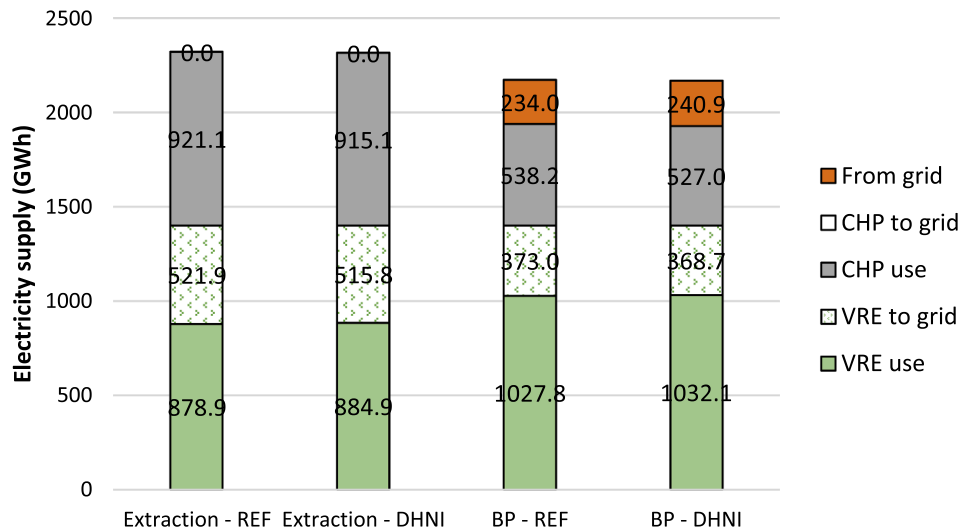


Fig. 12. Electricity supply of the extraction and back-pressure (BP) CHP systems.

Table 8

Storage efficiency and the effective conversion rate (ECR) of the DHNI in two systems.

Scenarios	Accumulated energy (GWh)		Storage Efficiency	Full-load Cycles	Improved VRE (GWh)	ECR
	Charge	Discharge				
Extraction	20.50	19.74	96.3%	134	6.0	0.31
Back-pressure	13.60	12.94	95.2%	88	4.3	0.33

Compared to the standalone energy storage unit such as the central water tank, the DH pipes are not only storage units but also the energy transportation carriers. Thus, the use of the storage capacity can be influenced by the fluctuations in the pipes. As for the back-pressure plant, although the heat-to-power ratio is near 4, the reduced power generating capacity has increased the VRE integrations, as explained hereafter.

The relatively small VRE integration benefit can also be explained by the limited usage of the DHNI during the low-demand period. As shown in Fig. 13, the optimization basically failed during summer because it is not economical feasible to raise network temperature to just shift a small

part of the load.

In the back-pressure plant, to actively raise the network supply water temperature, the saturated exhaust steam temperature is slightly increased from 100 °C to 110 °C. Consequently, the power generating capacity is reduced from 87.8 MW to 86.0 MW and the annual CHP power production is reduced by 11.2 GWh. As shown in Fig. 12, the reduced capacity can be partly fulfilled by the VRE, but the system still needs to buy electricity from the grid. Thus, although the use of VRE is increased by 4.3 MWh, the use of DHNI is not economically feasible in the BP system, as expressed by the total operational cost in Table 9. In comparison, the temperature of the extracted steam from the traditional extraction plant is high enough to heat up the network circulating water, with a little influence on the CHP plant efficiency. Thus, the total operating cost is reduced by 0.6% in the extraction system. Moreover, as shown in Table 8, the discharged energy in the BP system is also smaller than that in the extraction system because the optimization process failed for longer period due to the lowered BP plant efficiency.

However, the above results only refer to a certain scenario where the electricity demand is higher than the total power generating capacity of the CHP plant and the VRE. The benefits and potentials of the network storage are different as the balance between the VRE supply and electricity demand changes, which are further explained in Section 4.4.

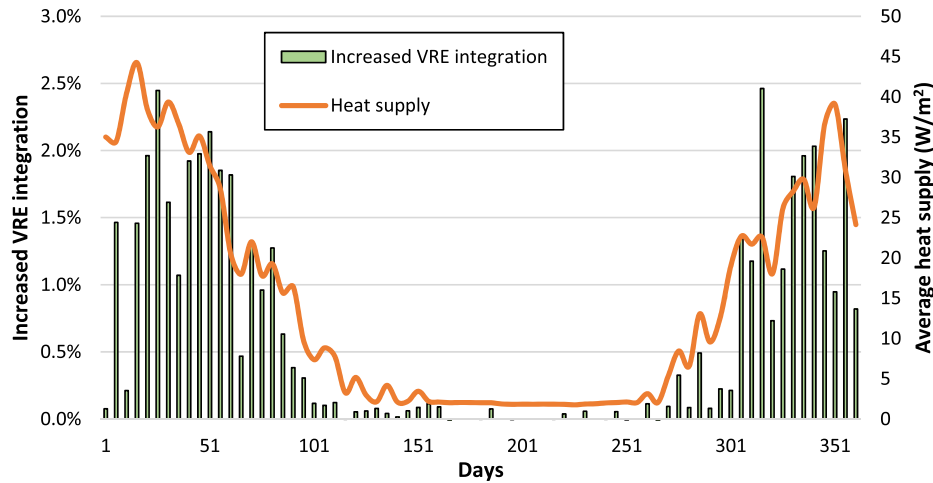


Fig. 13. Increased VRE integration rate in the extraction CHP system during the study year. Each bar represents one optimization cycle, which equals five days.

Table 9

Annual operational costs and fuel consumptions of the extraction and back-pressure CHP systems.

Scenarios	CHP Fuel (GWh)	Cost (million CNY)			
		Fuel cost	Grid bought	Pump	Total
Extraction - REF	2719	408	0	2.0	410
Extraction - DHNI	2705	406	0	2.0	408
Back-pressure - REF	3042	456	119	2.0	601
Back-pressure - DHNI	3040	456	123	2.0	605

4.2. LTDH scenarios

The extraction CHP plant is not preferable in LTDH systems due to its low exergy efficiency. Using the similar methodologies as in the previous section, the use of DHNI in the LTDH systems is modelled. The general results of improved VRE integration rates of different systems are summarized in Fig. 14. The cost-saving rate, which is the percentage of the saved money in annual operational cost, is also analyzed. For the system with back-pressure plant, as with the MTDH cases, the use of DHNI is economically infeasible since the electricity production is reduced.

As for the system with large-scale HPs, raising the network temperatures directly influences the HP efficiency. As shown in Table 10, the COPs are reduced, causing extra electricity consumptions for heating,

which cannot be offset by the improved VRE integrations. Thus, the operational cost becomes higher after using the DHNI. Indeed, the use of the DHNI is only feasible for 60 days, where the acquired benefits are larger than the loss of HP efficiencies. During the rest period, the operating cost is higher than that of the reference system. Thus, the DHNI can be only activated during the feasible period. The modelled results of this alternative scenario are also presented in Fig. 14 and Table 10, with a short name of LTDH - HP - feasible. With a shorter active adjusting period, the HP efficiencies are slightly influenced. Since the VRE integration benefits are also reduced, the general operating cost is only reduced by 0.05%.

The storage efficiencies and the ECRs for the DHNI in the three LTDH systems are summarized in Table 11. As explained above, taking only the feasible optimization period into account, the use of DHNI equals to 44 complete cycles, which is significantly lower than the other scenarios. Since the HP has higher heat-to-power ratio, the ECR index in the HP system is lower than the CHP systems. A qualitative analysis about the relationships between the ECR index and the benefits of thermal energy storage units can be found in the discussion part.

4.3. Influence of flowrate control strategies

The MTDH systems are used as case systems in this section to investigate the influence of the flowrate control strategy. As explained in section 2.2, due to the large transportation delay of the fixed flowrate

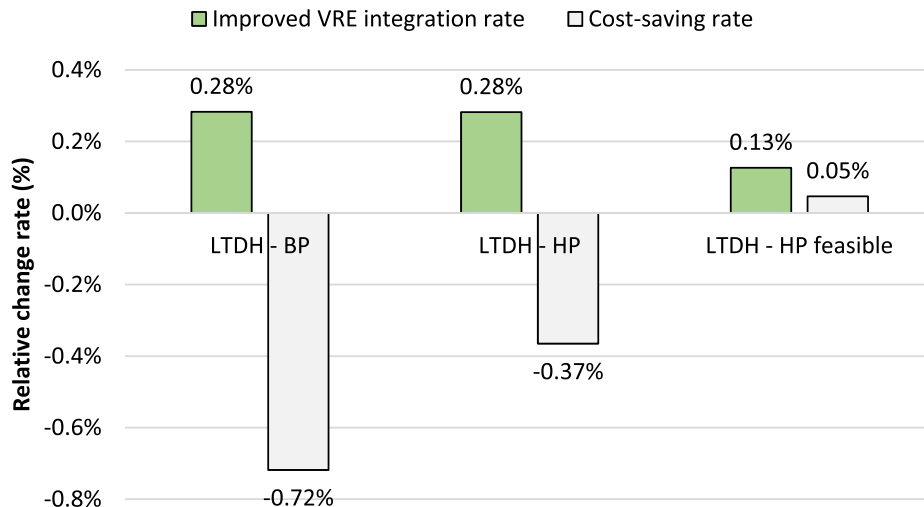


Fig. 14. Improved VRE integration rate and cost-saving rate for the LTDH systems with back-pressure (BP) CHP plant and HP as heating sources.

Table 10

Annual average COPs of the HPs and the improved VRE integrations in the LTDH systems.

Scenarios	COP	Average temperatures (°C)		Electricity demand (GWh)		VRE use (GWh)	Feasible days
		Supply	Return	Heating	Household		
LTDH - REF	4.89	55	26.8	120.6	1800	1175	–
LTDH - HP	4.64	59.2	27	128.5	1800	1180	60
LTDH - HP feasible	4.84	55.8	26.8	122.5	1800	1177	65

Table 11

Discharged energy of the DHNI and the storage performance.

Scenarios	Discharged energy (GWh)	Storage efficiency (%)	Equivalent cycles	ECR
LTDH - back pressure	15.8	93.7%	107	0.32
LTDH - HP	24.6	93.2%	167	0.21
LTDH - HP feasible	6.4	95.2%	44	0.35

strategy, the domestic hot water demand is currently omitted. The detailed supply and return water temperature profiles of the MTDH system with extraction CHP plant on Jan 4th are presented in Fig. 15, as an example. Compared to the variable flowrate strategy shown in Fig. 11, the storage capacities of the return pipes are utilized. Consequently, the discharged energy from the network inertia is increased on the annual level, as summarized in Table 12. However, the improved VRE integrations and associated cost-savings are not linearly increased with the discharged energy due to the limitations of the network storage capacity for handling intermittent VRE. Thus, the ECR indices are reduced to approximately 0.2. As for the MTDH system with back-pressure CHP plant, the VRE integration is also improved but the operating cost is still lower than the cost in the reference scenario.

The above strategy of fixed flowrate is only applicable in traditional DH systems, where the large transportation time lag is acceptable for merely the space heating demand. As the performance of the buildings is gradually improved, the instantaneous domestic hot water demand will play more important roles in the total heating demand [47,48], decreasing the feasibilities of the fixed flowrate control. Besides, with the widely acknowledged benefits from reducing the return water temperatures, using the inertia of the return pipes significantly impacts the heat source efficiency as indicated in the previous section, thus becoming infeasible from both the technical and economic aspects. Hence, the LTDH systems are not considered here.

Table 12

The improved VRE integrations and cost-savings of the MTDH systems with two control strategies for the whole study year.

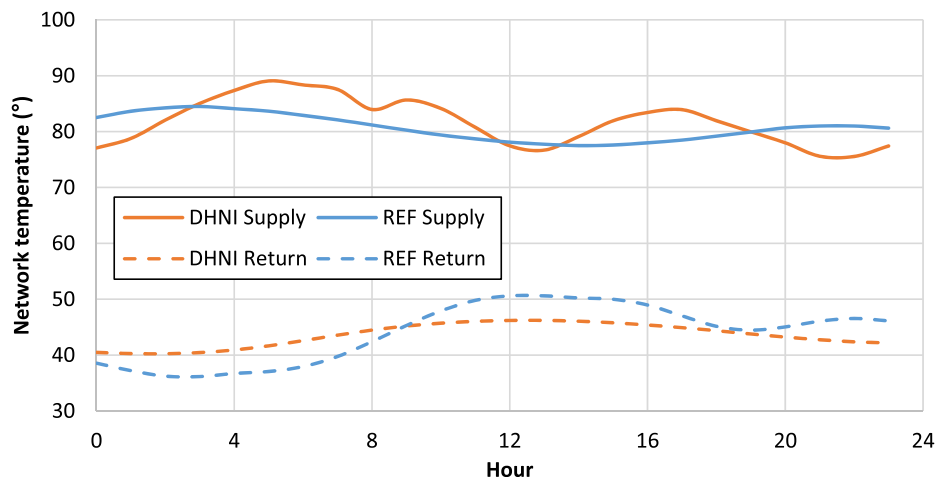
Source	Control strategy	Discharged energy (GWh)	Improved VRE		Cost saving	
			(GWh)	(%)	(Million CNY)	(%)
Extraction	Variable flowrate	19.7	6.0	0.4%	2.2	0.5%
	Fixed flowrate	44.0	8.9	0.6%	3.3	0.8%
Back-pressure	Variable flowrate	12.9	4.3	0.3%	−3.9	−0.7%
	Fixed flowrate	23.2	5.3	0.4%	−3.1	−0.5%

4.4. Influence of VRE balances

In addition to the scenarios explained above, various VRE supply profiles and household electric demand profiles are considered in the following to understand the benefits of the DHNI under different boundary conditions. The investigated scenarios are summarized in Table 4 and Table 5. The VRE scenarios represent the possible development of wind power in the future and the electric demand scenarios represent the boundaries of the investigated energy systems. Similarly to Section 4.3, the LTDH systems are not considered in this part due to the infeasibility of the DHNI.

Based on the simulated results, the key performance indicators for the use of the DHNI under the investigated scenarios, compared to the reference scenarios, are shown in Figs. 16–19. The ratio between the improved integrated VRE and the total supplied VRE, becomes smaller as the energy supply is larger. The capability of the network inertia to integrate VRE is also reflected in the ECR indicator, which has an upper limit due to the heat-to-power conversion efficiencies and the storage characteristics.

As for the system with extraction plant, although the economic benefits of the DHNI is increased with a larger VRE supply, upper limits of the cost-saving rate exist, which are approximately 0.7% and 0.6% for

**Fig. 15.** Network supply and return water temperatures for the MTDH system with fixed flowrate control strategy.

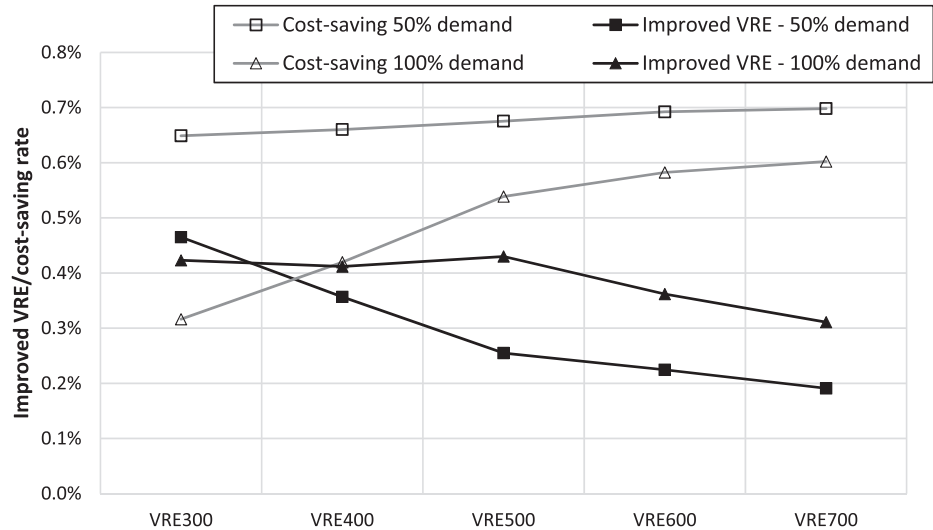


Fig. 16. Improved VRE integration rate and cost-saving rate for the MTDH systems with extraction plant under different conditions.

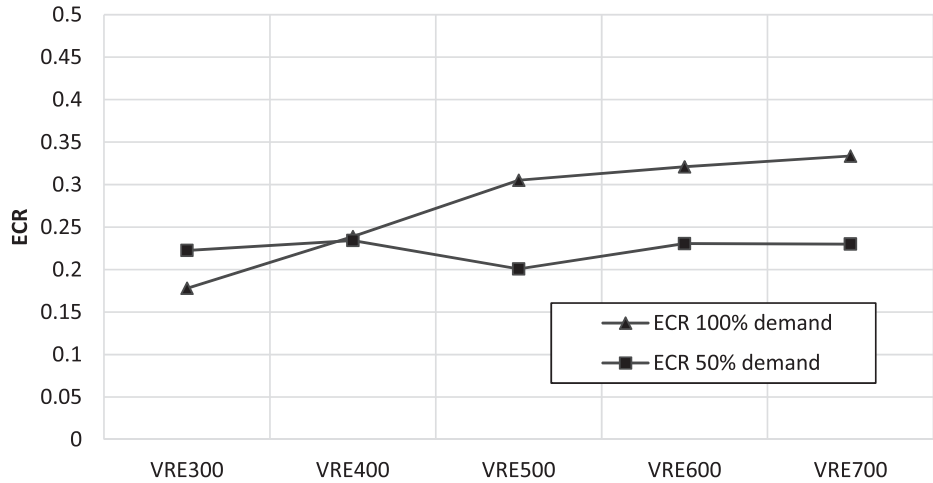


Fig. 17. Effective conversion ratio (ECR) for the DHNI in the MTDH systems with extraction plant.

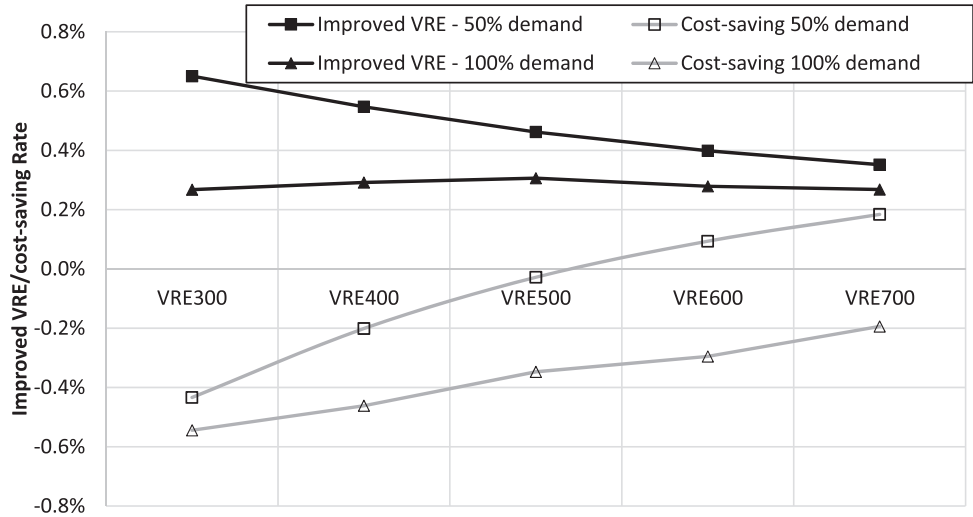


Fig. 18. Improved VRE integration rate and cost-saving rate for the MTDH systems with back-pressure plant under different conditions.

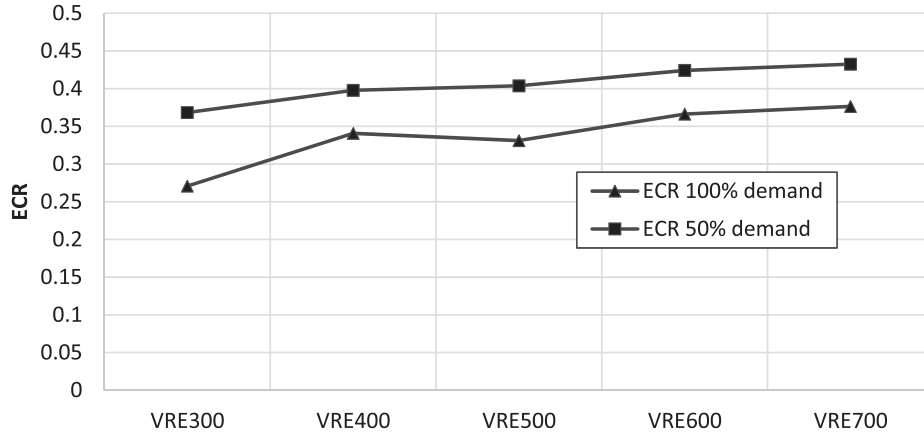


Fig. 19. Effective conversion ratio (ECR) for the DHNI in the MTDH systems with back-pressure plant.

the 50% demand and 100% demand scenarios, respectively. The upper limits are associated with the limitations to integrate the intermittent VRE. It is found that the use of the DHNI is only feasible in a certain range of application scenarios. Yet, the cost-saving benefit and VRE integration benefit are still relatively small, compared to the overall operating cost and energy consumptions of the studied whole system.

The ECR of the back-pressure plant is slightly higher than the extraction plant because the reduction of power generating capacity increases the VRE integrations, as explained in Table 9. Due to the same reason, the use of the DHNI in the back-pressure system is only economically feasible in the 50% demand scenario with VRE installed capacity larger than 600 MW. In this case, the installed capacity of the wind power is almost 6 times of the maximum power in the demand side, which is hard to be achieved in realistic systems.

4.5. Theoretical analysis of the storage usage

From the modelled results presented in above sections, it is found that even under the most favorable scenario, the VRE integration benefit of the DHNI is still relatively small compared to the overall energy productions and consumptions. To explore the reasons behind this result, theoretical breakdown analysis of the effective usage of the storage unit is conducted, as shown in Fig. 20. The analysis process is expressed in Eq. (14). Alternatively, the ECR index can be written as Eq. (15).

Considering a system with 100% electricity demand and 100% heating demand in Fig. 20, the design storage capacity of the TES unit is expressed by θ_{TES} , which is for example 5% of the heating demand according to the investigation results in Section 3. Then, by including practical limitation in terms of heat losses and control precisions, expressed by $\eta_{heatloss}$ and $\eta_{control}$ respectively, a usable part of the storage capacity is identified. This part is then converted to shift the electric load with a heat-to-power conversion factor η_{h2p} , which usually has values of 2 for extraction CHP plant and between 3 and 5 for HPs. By dividing the η_{h2p} , the final converted electricity $\theta_{el,shift}$ becomes even smaller, i.e. 1.7% as shown in Fig. 20. If the energy system has higher electricity demand, such as the baseline system where the electricity demand is three times of the heating demand, the benefit of the converted electricity becomes less significant.

In the above analysis, the heat loss coefficient $\eta_{heatloss}$ is influenced by the thermal characteristics of the storage unit and has a range of 80% to 95%. The control precision $\eta_{control}$ is a rather complex index that is decided by various factors such as the location of the storage unit, the system complexity and the load fluctuations, as explained in Section 4.1. The heat-to-power factor, η_{h2p} , is directly related to the heat sources, which are designed according to the whole energy system plans. Using the above method, the load shifting benefit of the storage unit can be theoretically assessed.

$$\theta_{el,shift} = \theta_{TES} * \eta_{heatloss} * \eta_{control} / \eta_{h2p} \quad (14)$$

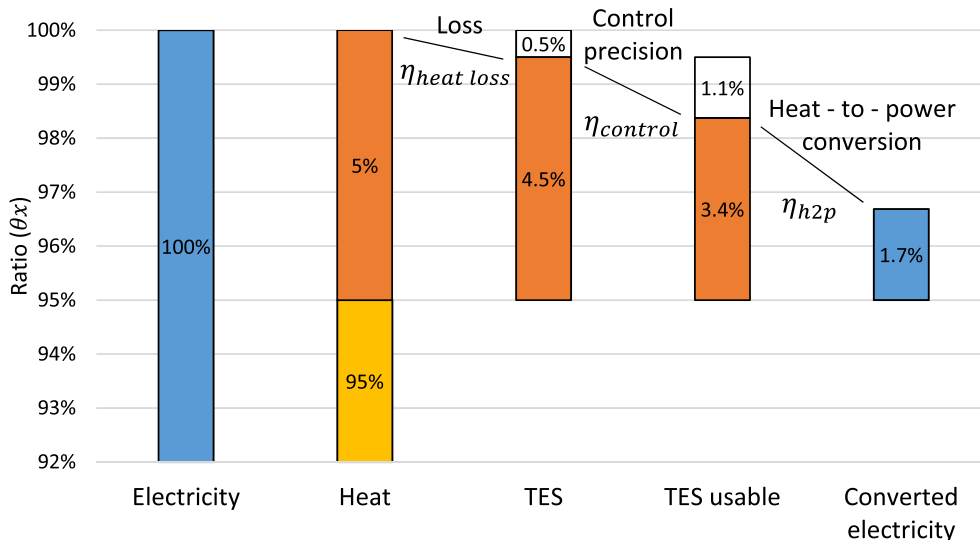


Fig. 20. Breakdown analysis of the effective usage of the TES for electric load shifting.

$$ECR = \eta_{\text{heatloss}}^* \eta_{\text{control}} / \eta_{\text{h2p}} \quad (15)$$

5. Discussion

In this study, the benefits of the DHNI are derived from the comparison of the reference scenario and the active-controlled scenario. The reference scenario is assumed to have a theoretical control over the flowrate so that the network inertia is not used at all. However, in reality, due to the time delays in almost all parts of the complex DH system, the practical control strategy can hardly reach the theoretically assumed one. Therefore, the network inertia is unavoidable utilized to some levels, causing positive or even negative effects on the system performance and operating costs. Since the exact time delays and practical performance are hard to modelled, the results of this study are only limited to theoretical assumptions.

Various methods have been developed in recent years to recycle the waste heat from the exhaust steam and to increase plant efficiency [44], such as the use of the absorption heat pump [49]. However, these improvements are not considered for the extraction CHP plant in this study. Taking the system with the absorption heat pump as an example, the amount of the extracted steam and exhaust steam shall be carefully controlled, to match the high-grade and low-grade energy sources. Thus, the use of the extracted steam to raise the network temperatures might impact the overall system efficiency. The applicability of the DHNI in the newly developed CHP systems shall be further examined. Moreover, flexible heat storage options such as the two tanks design [50], have been developed in recent years to improve system flexibility while fully recovering the waste heat.

6. Conclusion

This study has investigated the storage potentials of the DH pipes in a group of representative DH systems in Sweden and China with different load densities. Based on an integrated DH system model, developed in-house, the technical and economical feasibilities for using the network inertia as storage unit are analyzed under various scenarios, including the different network temperature levels, heat sources, flowrate control strategies and the VRE balances. The suitable application ranges and the proposed benefits of using the network inertia are found thereby. Key conclusions are summarized as follows:

- (1) The investigations of the DH systems have shown that the storage capacities of the studied Swedish DH networks are always less than 0.8% of the daily heating demand, considering a 10 K temperature increase in the supply network. In contrary, due to over-sized pipes, the same index in Chinese DH systems is on average 4% of the daily heating demand.
- (2) In traditional MTDH systems with the extraction CHP plant, since the heat source efficiency is not influenced by the raised network temperatures, the DHNI can improve the VRE integrations by 0.4% of the total VRE supply and reduce the total operating cost by 0.6%. In the scenario with the back-pressure plant, although the integrations of VRE is improved, the use of DHNI is not economically attractive because the system needs to buy more electricity from the grid.
- (3) In future LTDH systems with HPs, the DHNI is only feasible for a short period due to reduced source efficiencies, leading to a small cost-saving rate of 0.05%. In LTDH systems with back-pressure plants, the DHNI is still economically infeasible as is in the MTDH systems.
- (4) The fixed flowrate control strategy can better utilize the storage capacity compared to the variable flowrate strategy. By changing the VRE supply and electricity demand profiles, the upper limits of the cost-saving benefits for utilizing the DHNI are found, along

with the upper limits of the effective conversion ratios between the storage capacity and the shifted electric load.

Finally, theoretical breakdown analysis of the effective usage of the storage unit is conducted, to explain the relatively small benefit associated with the network inertia. The proposed analysis method can be applied to all TES units. From the results of this study, it is pointed out that the DHNI can only play limited roles for improving the flexibility in future DH systems.

Declaration of Competing Interest

The authors declare that they have no known competing financial interests or personal relationships that could have appeared to influence the work reported in this paper.

Acknowledgement

This work was supported by the Swedish Research Council for Environment, Agricultural Sciences and Spatial Planning (FORMAS) [Grant No. 2018-01228]. The authors also thank the Chalmers Energy Area of Advance, Profile area: Energy in Urban Development for the additional financial support. The authors would like to express sincere thanks to the DH companies for providing operational data and network information.

References

- [1] P.D. Lund, J. Lindgren, J. Mikkola, J. Salpakari, Review of energy system flexibility measures to enable high levels of variable renewable electricity, *Renew. Sustain. Energy Rev.* 45 (2015) 785–807, <https://doi.org/10.1016/j.rser.2015.01.057>.
- [2] D. Gielen, F. Boshell, D. Saygin, M.D. Bazilian, N. Wagner, R. Gorini, The role of renewable energy in the global energy transformation, *Energy Strateg. Rev.* 24 (2019) 38–50, <https://doi.org/10.1016/j.esr.2019.01.006>.
- [3] M.I. Alizadeh, M. Parsa Moghaddam, N. Amjadi, P. Siano, M.K. Sheikh-El-Eslami, Flexibility in future power systems with high renewable penetration: A review, *Renew. Sustain. Energy Rev.* 57 (2016) 1186–1193, <https://doi.org/10.1016/j.rser.2015.12.200>.
- [4] H. Lund, P.A. Østergaard, D. Connolly, B.V. Mathiesen, Smart energy and smart energy systems, *Energy* 137 (2017) 556–565, <https://doi.org/10.1016/j.energy.2017.05.123>.
- [5] H. Lund, P.A. Østergaard, M. Chang, S. Werner, S. Svendsen, P. Sorknæs, J. E. Thorsen, F. Hvelplund, B.O.G. Mortensen, B.V. Mathiesen, C. Bojesen, N. Duic, X. Zhang, B. Möller, The status of 4th generation district heating: Research and results, *Energy* 164 (2018) 147–159.
- [6] H. Lund, P.A. Østergaard, D. Connolly, B.V. Mathiesen, Energy storage and smart energy systems, *Energy* 137 (2017) 556–565, <https://doi.org/10.1016/j.energy.2017.05.123>.
- [7] S. Buffa, M. Cozzini, M. D'Antoni, M. Baratieri, R. Fedrizzi, 5th generation district heating and cooling systems: A review of existing cases in Europe, *Renew. Sustain. Energy Rev.* 104 (2019) 504–522, <https://doi.org/10.1016/j.rser.2018.12.059>.
- [8] N.J. Hewitt, Heat pumps and energy storage - The challenges of implementation, *Appl. Energy* 89 (2012) 37–44, <https://doi.org/10.1016/j.apenergy.2010.12.028>.
- [9] A. David, B.V. Mathiesen, H. Averfalk, S. Werner, H. Lund, Heat Roadmap Europe: Large-scale electric heat pumps in district heating systems, *Energies* 10 (2017) 1–18, <https://doi.org/10.3390/en10040578>.
- [10] H. Gadd, S. Werner, Thermal energy storage systems for district heating and cooling, Woodhead Publishing Limited; 2015. <https://doi.org/10.1533/9781782420965.4.467>.
- [11] E. Guelpa, V. Verda, Thermal energy storage in district heating and cooling systems: A review, *Appl. Energy* 252 (2019), 113474, <https://doi.org/10.1016/j.apenergy.2019.113474>.
- [12] J. Hennessy, H. Li, F. Wallin, E. Thorin, Flexibility in thermal grids: A review of short-term storage in district heating distribution networks, *Energy Procedia* 158 (2019) 2430–2434, <https://doi.org/10.1016/j.egypro.2019.01.302>.
- [13] D. Basciotti, F. Judez, O. Pol, R.-R. Schmidt, Sensible heat storage in district heating networks: a novel control strategy using the network as storage. IRES - 6th Int Renew Energy Storage Conf Exhib, 2011.
- [14] H. Lund, Renewable heating strategies and their consequences for storage and grid infrastructures comparing a smart grid to a smart energy systems approach, *Energy* 151 (2018) 94–102, <https://doi.org/10.1016/j.energy.2018.03.010>.
- [15] H. Lund, Corrigendum to "Renewable heating strategies and their consequences for storage and grid infrastructures comparing a smart grid to a smart energy systems approach" [*Energy* 151 (2018) 94–102], *Energy* 153 (2018) 1087.
- [16] W. Zheng, J.J. Hennessy, H. Li, Reducing renewable power curtailment and CO2 emissions in China through district heating storage, *Wiley Interdiscip. Rev. Energy Environ.* 9 (2020) 1–11, <https://doi.org/10.1002/wene.361>.

- [17] S. Frederiksen, S. Werner, District heating and cooling, *Studentlitteratur*. AB (2013).
- [18] J. Zheng, Z. Zhou, J. Zhao, J. Wang, Integrated heat and power dispatch truly utilizing thermal inertia of district heating network for wind power integration, *Appl. Energy* 211 (2018) 865–874, <https://doi.org/10.1016/j.apenergy.2017.11.080>.
- [19] J. Wang, Z. Zhou, J. Zhao, J. Zheng, Improving wind power integration by a novel short-term dispatch model based on free heat storage and exhaust heat recycling, *Energy* 160 (2018) 940–953, <https://doi.org/10.1016/j.energy.2018.07.018>.
- [20] Z. Li, W. Wu, M. Shahidehpour, J. Wang, B. Zhang, Combined heat and power dispatch considering pipeline energy storage of district heating network, *IEEE Trans. Sustain. Energy* 7 (2016) 12–22, <https://doi.org/10.1109/TSTE.2015.2467383>.
- [21] W. Gu, J. Wang, S. Lu, Z. Luo, C. Wu, Optimal operation for integrated energy system considering thermal inertia of district heating network and buildings, *Appl. Energy* 199 (2017) 234–246, <https://doi.org/10.1016/j.apenergy.2017.05.004>.
- [22] X. Huang, Z. Xu, Y. Sun, Y. Xue, Z. Wang, Z. Liu, Z. Li, W. Ni, Heat and power load dispatching considering energy storage of district heating system and electric boilers, *J. Mod. Power. Syst. Clean. Energy* 6 (5) (2018) 992–1003.
- [23] J. Zheng, Z. Zhou, J. Zhao, J. Wang, Effects of the operation regulation modes of district heating system on an integrated heat and power dispatch system for wind power integration, *Appl. Energy* 230 (2018) 1126–1139, <https://doi.org/10.1016/j.apenergy.2018.09.077>.
- [24] J. Salpakari, J. Mikkola, P.D. Lund, Improved flexibility with large-scale variable renewable power in cities through optimal demand side management and power-to-heat conversion, *Energy Convers. Manage.* 126 (2016) 649–661, <https://doi.org/10.1016/j.enconman.2016.08.041>.
- [25] J. Mikkola, P.D. Lund, Modeling flexibility and optimal use of existing power plants with large-scale variable renewable power schemes, *Energy* 112 (2016) 364–375, <https://doi.org/10.1016/j.energy.2016.06.082>.
- [26] D. Balić, D. Maljković, D. Lončar, Multi-criteria analysis of district heating system operation strategy, *Energy Convers. Manage.* 144 (2017) 414–428, <https://doi.org/10.1016/j.enconman.2017.04.072>.
- [27] T. Korpela, J. Kaivosoja, Y. Majanne, L. Laakkonen, M. Nurmoranta, M. Vilkkö, Utilization of district heating networks to provide flexibility in CHP Production, *Energy Procedia* 116 (2017) 310–319, <https://doi.org/10.1016/j.egypro.2017.05.077>.
- [28] M. Turski, R. Sekret, Buildings and a district heating network as thermal energy storages in the district heating system, *Energy Build* 179 (2018) 49–56, <https://doi.org/10.1016/j.enbuild.2018.09.015>.
- [29] H. Lund, S. Werner, R. Wiltshire, S. Svendsen, J.E. Thorsen, F. Hvelplund, B. V. Mathiesen, 4th Generation District Heating (4GDH) Integrating smart thermal grids into future sustainable energy systems, *Energy* 68 (2014) 1–11.
- [30] H. Averfalk, S. Werner, Economic benefits of fourth generation district heating, *Energy* 193 (2020), 116727, <https://doi.org/10.1016/j.energy.2019.116727>.
- [31] Y. Zhang, P. Johansson, A.S. Kalagasidis, Applicability of thermal energy storage in future low-temperature district heating systems – Case study using multi-scenario analysis, *Energy Convers. Manage.* 244 (2021) 114518.
- [32] Y. Li, J. Xia, H. Fang, Y. Su, Y. Jiang, Case study on industrial surplus heat of steel plants for district heating in Northern China, *Energy* 102 (2016) 397–405, <https://doi.org/10.1016/j.energy.2016.02.105>.
- [33] Ministry of Housing Urban-Rural Development, Standard for Energy consumption of Building GB/T 51161–2016, Architecture and Building Press, Beijing, China, 2016.
- [34] Ministry of Housing Urban-Rural Development, JGJ 26–95 Energy conservation design standard for new heating residential buildings, Architecture and Building Press, Beijing, China, 1995.
- [35] Ministry of Housing Urban-Rural Development, JGJ 26–2010 Design Standard for Energy Efficiency of Residential Buildings in Severe Cold and Cold Zones, Architecture and Building Press, Beijing, China, 2010.
- [36] X.C. Fan, W.Q. Wang, R.J. Shi, F.T. Li, Analysis and countermeasures of wind power curtailment in China, *Renew. Sustain. Energy Rev* 52 (2015) 1429–1436, <https://doi.org/10.1016/j.rser.2015.08.025>.
- [37] J. Chen, H. Cui, Y. Xu, Q. Ge, Long-term temperature and sea-level rise stabilization before and beyond 2100: Estimating the additional climate mitigation contribution from China's recent 2060 carbon neutrality pledge, *Environ. Res. Lett* 16 (7) (2021) 074032.
- [38] de Normalización CE. EN ISO 13790: Energy Performance of Buildings: Calculation of Energy Use for Space Heating and Cooling (ISO 13790: 2008). CEN; 2008.
- [39] U. Jordan, K. Vajen, Realistic domestic hot-water profiles in different time scales, in: Rep Sol Heat Cool Progr Int Energy Agency (IEA-SHC)Task, 2001, pp. 1–18.
- [40] A. Benonysson, B. Böhm, H.F. Ravn, Operational optimization in a district heating system, *Energy Convers. Manage.* 36 (5) (1995) 297–314.
- [41] H. Zhao, Analysis, modelling and operational optimization of district heating systems [J] 1995. <https://www.osti.gov/etdweb/biblio/78473>.
- [42] Y. Zhang, J. Xia, H. Fang, Y. Jiang, Z. Liang, Field tests on the operational energy consumption of Chinese district heating systems and evaluation of typical associated problems, *Energy Build.* 224 (2020), 110269, <https://doi.org/10.1016/j.enbuild.2020.110269>.
- [43] R. Lahdelma, H. Hakonen, An efficient linear programming algorithm for combined heat and power production, *Eur. J. Oper. Res.* 148 (2003) 141–151, [https://doi.org/10.1016/S0377-2217\(02\)00460-5](https://doi.org/10.1016/S0377-2217(02)00460-5).
- [44] Y. Li, S. Chang, L. Fu, S. Zhang, A technology review on recovering waste heat from the condensers of large turbine units in China, *Renew. Sustain. Energy Rev.* 58 (2016) 287–296, <https://doi.org/10.1016/j.rser.2015.12.059>.
- [45] M. Maivel, J. Kurnitski, Heating system return temperature effect on heat pump performance, *Energy Build.* 94 (2015) 71–79, <https://doi.org/10.1016/j.enbuild.2015.02.048>.
- [46] U. Persson, S. Werner, Heat distribution and the future competitiveness of district heating, *Appl. Energy* 88 (2011) 568–576, <https://doi.org/10.1016/j.apenergy.2010.09.020>.
- [47] H. Braas, U. Jordan, I. Best, J. Orozaliyev, K. Vajen, District heating load profiles for domestic hot water preparation with realistic simultaneity using DHWcalc and TRNSYS, *Energy* 201 (2020), 117552, <https://doi.org/10.1016/j.energy.2020.117552>.
- [48] H. Averfalk, S. Werner, Novel low temperature heat distribution technology, *Energy* 145 (2018) 526–539, <https://doi.org/10.1016/j.energy.2017.12.157>.
- [49] Y. Li, L. Fu, S. Zhang, Y. Jiang, Z. Xiling, A new type of district heating method with co-generation based on absorption heat exchange (co-ah cycle), *Energy Convers. Manage.* 52 (2011) 1200–1207, <https://doi.org/10.1016/j.enconman.2010.09.015>.
- [50] Y. Wu, L. Fu, S. Zhang, D. Tang, Study on a novel co-operated heat and power system for improving energy efficiency and flexibility of cogeneration plants, *Appl. Therm. Eng.* 163 (2019), 114429, <https://doi.org/10.1016/j.applthermaleng.2019.114429>.